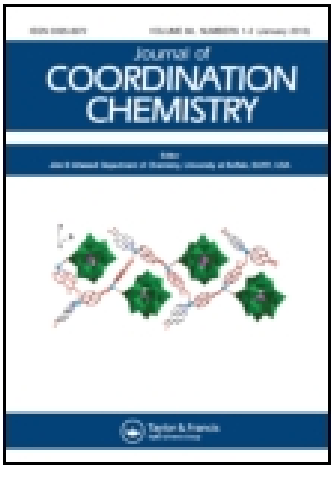

Journal of Coordination Chemistry
Publication details, including instructions for authors and subscription information:
http://www.tandfonline.com/loi/gcoo20

A new 1-D energetic complex $[Cu(2,3'\text{-bpt})_2 \cdot H_2O]_n$: synthesis, structure, and catalytic thermal decomposition for ammonium perchlorate

Bing Li[a], Dan Shen[a], Xiaoyan Chen[a], Ting Li[a], Jianlin Ren[a], Qilin Hu[a] & Wanyi Liu[a]

[a] Department of Chemistry and Chemical Engineering, Ningxia University, Yinchuan, PR China

Accepted author version posted online: 16 Jun 2014.Published online: 14 Jul 2014.

Journal of Coordination Chemistry, 2014
Vol. 67, No. 11, 2028–2038, http://dx.doi.org/10.1080/00958972.2014.934230

A new 1-D energetic complex $[Cu(2,3'\text{-bpt})_2 \cdot H_2O]_n$: synthesis, structure, and catalytic thermal decomposition for ammonium perchlorate

BING LI*, DAN SHEN, XIAOYAN CHEN, TING LI, JIANLIN REN, QILIN HU and WANYI LIU

Department of Chemistry and Chemical Engineering, Ningxia University, Yinchuan, PR China

(*Received 5 October 2013; accepted 16 May 2014*)

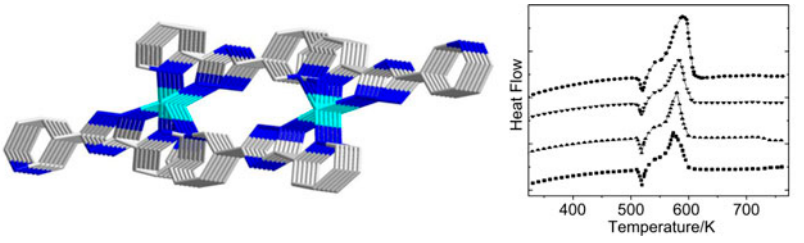

A new energetic complex, $[Cu(2,3'\text{-bpt})_2 \cdot H_2O]_n$, displays a 1-D channel in the *ac* plane and further links into 2-D planes by the hydrogen-bond interactions. AP is completely decomposed in a shorter time and releases more heat in the presence of complex **1**. By Kissinger's method, the ratio of $E_a/\ln(A)$ is 12.23 for the mixture, which indicates that complex **1** shows good catalytic activity toward AP decomposition.

A new energetic complex, $[Cu(2,3'\text{-bpt})_2 \cdot H_2O]_n$ (**1**) (2,3′-Hbpt = 3-(2-pyridyl)-5-(3′-pyridyl)1H-1,2,4-triazole), was synthesized and characterized by single-crystal X-ray diffraction, thermogravimetric analyses, elemental analysis, X-ray powder diffraction, and IR spectroscopy. The title complex belongs to the monoclinic system, space group $P2_1/c$. In the complex, one 2,3′-bpt$^-$ is a chelate binding to Cu(II) centers forming a Cu(2,3′-bpt)$^+$ unit. Then the other 2,3′-bpt$^-$ adopts chelate/bridging tridentate mode linking adjacent Cu(2,3′-bpt)$^+$ units to a zigzag chain along the (110) direction and a 1-D channel in the *ac* plane. Hydrogen-bond interactions link the channels into 2-D planes. The thermal decomposition of ammonium perchlorate (AP) with **1** was explored by differential scanning calorimetry from 323 to 773 K. AP is completely decomposed in a shorter time in the presence of **1**, and the decomposition heat of the mixture is 1946 J g^{-1}, significantly higher than pure AP. By Kissinger's method, the ratio of $E_a/\ln(A)$ is 12.23 for the mixture, which indicates that **1** shows good catalytic activity toward AP decomposition.

Keywords: Energetic; 2,3′-Hbpt; Crystal structure; Catalytic thermal decomposition

*Corresponding author. Email: libing@nxu.edu.cn

1. Introduction

With the development of energetic materials, high-energy density materials have attracted attention [1–5]. Nitrogen-rich compounds rely on their highly efficient gas production and high heat of formation for energy release, since elemental nitrogen, which has a zero heat of formation, is the major product of decomposition [6, 7]. These compounds are prospective materials for generation of gasses as blowing agents, solid propellants, and other combustible and thermally decomposing systems [8]. 3-(2-pyridyl)-5-(3′-pyridyl)-1H-1,2,4-triazole (2,3′-Hbpt) is one of the energetic ligands and their complexes can be used as energetic materials. 2,3′-Hbpt can serve as an N,N′-donor and act as a bridge, thus mediating exchange coupling [9–12]. The prototropy and conjugation among the 1H-1,2,4-triazole and pyridyl groups not only alter the electron density in different sections of the molecules, but make the ligand more flexible [13, 14]. Salts of Hbpt exhibit the potential application as additives in pyrotechnics and propellants. However, salts of Hbpt as additives in propellants are rarely reported.

Ammonium perchlorate (AP) is the common oxidizer which has been widely used in the main component of solid rocket propellant. The thermal decomposition characteristics of AP directly influence the combustion behavior of solid propellants [15, 16]. Many effective combustion catalysts on the thermal decomposition of AP, such as metal oxides which are not nitrogen-rich or energetic compounds, have been reported [17–20]. We anticipate a complex of Hbpt would not only provide fresh metal or metal oxide at the molecular level, but also give absorbing structure and greater heat of formation, which may improve the thermolysis of AP when the compounds are used as additives [21].

Our research group is interested in Hbpt and its derivatives for the syntheses of polymeric compounds with transition metals as well as the energetic characteristics for these compounds [7, 9, 22, 23]. As further investigation of energetic materials based on 2,3′-Hbpt, we report the synthesis, crystal structure, and thermal properties of $[Cu(2,3'\text{-bpt})_2 \cdot H_2O]_n$. The catalytic performances of **1** on AP decomposition are also studied, which shows **1** can accelerate the decomposition of AP.

2. Experimental

2.1. *Chemicals and apparatus*

All reagents for the syntheses were purchased from Tokyo Kasti Kogyo Co. Ltd. and were of analytical reagent (AR) grade with a purity of 99%.

Elemental analyses (C, H, and N) were performed on a Vario EL III analyzer. ^{1}H NMR spectra were taken with a Varian 400 spectrometer using tetramethylsilane as an internal standard. Infrared spectra were obtained from KBr pellets on a BEQ VZNDX 550 FTIR instrument from 400 to 4000 cm^{-1}. TG-DTG experiment was performed on a NETZSCH STA 449C thermal analyzer with a heating rate of 10 K min^{-1} under static air from 323 to 1050 K. The differential scanning calorimetry (DSC) experiment was performed on the thermal analyzer of Perkin-Elmer Pyris 6 DSC (calibrated by standard pure indium and zinc) with a heating rate of 5, 10, 15, and 20 K min^{-1} from 323 to 773 K.

Single-crystal X-ray experiment was performed on a Bruker Smart Apex charge-coupled device diffractometer with graphite monochromated Mo Kα radiation ($\lambda = 0.71073$ Å) using

Table 1. Crystal data and structure refinement parameters for **1**.

Empirical formula	$C_{24}H_{18}CuN_{10}O$
Formula weight	526.02
Crystal system	Monoclinic
Space group	$P2_1/c$
a (Å)	11.808(4)
b (Å)	9.828(3)
c (Å)	21.109(5)
α (°)	90
β (°)	112.859(14)
γ (°)	90
Z	4
D_{Calcd} (mg m^{-3})	1.548
F (0 0 0)	1076
Theta range for data collection (°)	1.87–24.25
Absorption coefficient (mm^{-1})	1.009
Reflections collected/unique	8216/3231
Final R indices [$I > 2\sigma(I)$]	$R_1 = 0.0759$, $wR_2 = 0.1454$
R indices (all data)	$R_1 = 0.1884$, $wR_2 = 0.1949$
Largest diff. peak and hole (e Å^3)	0.539 and −0.375

Table 2. Selected bond lengths (Å) and angles (°) for **1**.

Bond lengths			
N(5)–Cu(1)#1	2.341(8)	Cu(1)–N(1)	2.040(8)
Cu(1)–N(2)	1.945(8)	Cu(1)–N(6)	2.050(8)
Cu(1)–N(7)	1.962(8)	Cu(1)–N(5)#2	2.341(8)
Bond angles			
N(2)–Cu(1)–N(7)	167.2(3)	N(1)–Cu(1)–N(6)	170.9(3)
N(2)–Cu(1)–N(1)	80.2(4)	N(2)–Cu(1)–N(5)#2	98.9(3)
N(7)–Cu(1)–N(1)	99.2(4)	N(7)–Cu(1)–N(5)#2	93.9(3)
N(2)–Cu(1)–N(6)	98.7(4)	N(1)–Cu(1)–N(5)#2	95.8(3)
N(7)–Cu(1)–N(6)	79.9(4)	N(6)–Cu(1)–N(5)#2	93.3(3)

Note: Symmetry operations: #1 $-x+1, y+1/2, -z+1/2$; #2 $-x+1, y-1/2, -z+1/2$.

ω and φ scan modes. The single-crystal structure was solved by direct methods and refined with full-matrix least-squares refinement based on F^2 using SHELXS 97 and SHELXL 97. All non-H atoms were located using subsequent Fourier difference methods. In all cases, hydrogens were placed in calculated positions and thereafter allowed to ride on their parent atoms. Other details of crystal data, data collection parameters, and refinement statistics are given in table 1. Selected bond distances and angles are given in table 2.

2.2. *Synthesis of complex*

2,3′-Hbpt was synthesized according to [24] and further proved by elemental analysis, IR, and ^{1}H NMR. Anal. Calcd for $C_{12}H_9N_5$ (%): C, 64.56; H, 4.06; N, 31.37. Found: C, 64.96; H, 4.40; N, 32.45. M.p.: (528–529) K; IR (cm^{-1}, KBr): 3327(s), 3156(s), 3048(m), 2843(m), 1620(s), 1594(s), 1482(w), 1406(s), 1308(s), 1196(w), 1051(m), 821(m), 709(m), 625(w). ^{1}H NMR(400 MHz, DMSO-d$_6$, δppm): 6.988(s, 1H), 7.49–7.54 (q, $J = 8.4$ Hz, 1H), 7.92–7.93 (*t*, $J = 7.6$ Hz, 1H), 8.19 (d, $J = 7.6$ Hz, 1H), 8.23 (d, $J = 8.0$ Hz, 1H), 8.62 (d, $J = 4.4$ Hz, 1H), 8.72 (d, $J = 3.6$ Hz, 1H), 9.04 (s, 1H), 10.34 (s, 1H).

Synthesis of $[Cu(2,3'\text{-bpt})_2 \cdot H_2O]_n$: a mixture containing $Cu(OAc)_2 H_2O$ (19.9 mg, 0.10 mM), 2,3′-Hbpt (33.6 mg, 0.15 mM), and water (6 mL) was sealed in a 15 mL Teflon-lined stainless steel vessel, which was heated at 443 K for three days and then cooled to room temperature at a rate of 2 K h^{-1}. Blue prism crystals of **1** were collected

in a yield of 48% (based on Cu). Anal. Calcd for **1** ($C_{24}H_{18}CuN_{10}O$) (%): C, 54.80; H, 3.45; N, 26.63. Found: C, 54.61; H, 3.57; N, 26.31. IR (cm^{-1}, KBr): 3376(m), 3024(m), 1610(s), 1550(s), 1484(s), 1450(s), 1399(s), 1368(m), 1230(m), 1020(s), 835(m), 771(m), 701(s), 506(m).

3. Results and discussion

3.1. *Crystal structure of $[Cu(2,3'\text{-bpt})_2H_2O]_n$*

Single-crystal X-ray analysis shows that **1** has a 1-D array structure. As shown in figure 1, the asymmetric unit of **1** has one crystallographically independent Cu(II) center, two 2,3′-bpt ligands, and one uncoordinated water, displaying a slightly distorted tetragonal pyramidal geometry. Five-coordinate copper(II) complexes usually have tetragonal pyramidal vs. trigonal bipyramidal stereochemistries. Ideally, tetragonal pyramidal geometry is associated with bond angles of 90° in the square. While in the great majority of real tetragonal–pyramidal systems, metal center is displaced out of the square which makes the bond angles less than 90°. Trigonal bipyramidal stereochemistry is associated with the bond angles about 120° with the metal center in the triangular square. The bond angles and the position of copper(II) center of the title complex match the characteristics of tetragonal–pyramidal stereochemistry. The equatorial square is composed of N2 and N7 from the triazole rings, and N1 and N6 from the pyridine rings. The apical position is occupied by N5 from pyridine from 2,3′-bpt^-. The Cu–N bond lengths range from 1.962(8) to 2.341(8) Å and the N···Cu···N bond angles range from 79.9(4)° to 170.9(4)°, which are all in normal ranges. Completely deprotonated two 2,3′-bpt^- ligands display different coordination modes. One 2,3′-bpt^- is a chelate forming a Cu(2,3′-bpt)$^+$ unit and the two terminal pyridine rings of 2,3′-bpt are slightly twisted by 11.18°. The other 2,3′-bpt^- is chelate/bridging tridentate linking adjacent Cu(2,3′-bpt)$^+$ units to a zigzag chain along the (110) direction (figure 2) and two terminal pyridine rings are twisted with a dihedral angle of 17.68°. Comparing to our previous work [9] on 2,3′-Hbpt, not only the nitrogens from 2′-pyridyl and triazole, but also the nitrogen from 3′-pyridyl coordinate. All 2,3′-bpt^- are chelate ligands that bind to cobalt forming a 0-D motif in our previous work, while 2,3′-bpt^- in the title complex adopts chelate and chelate/bridging tridentate modes binding to copper forming a 1-D channel in the *ac* plane (figure 3). The different coordination modes are the key reasons for the structural diversity.

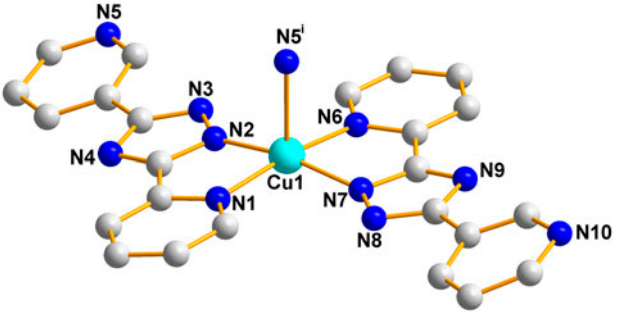

Figure 1. The molecular structure of **1**.

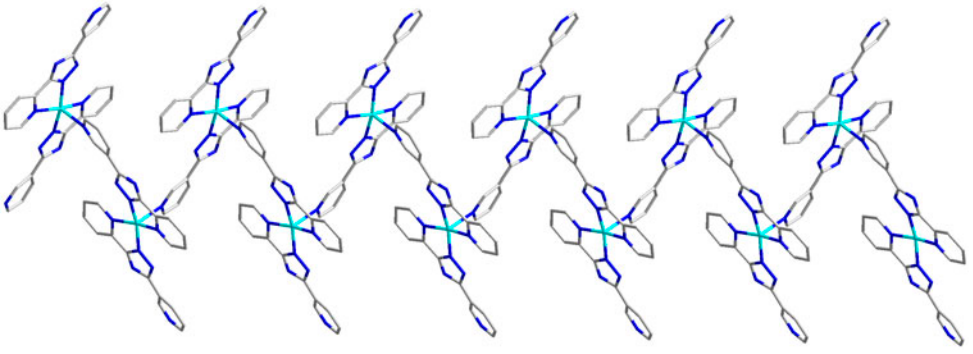

Figure 2. The zigzag chain of **1**.

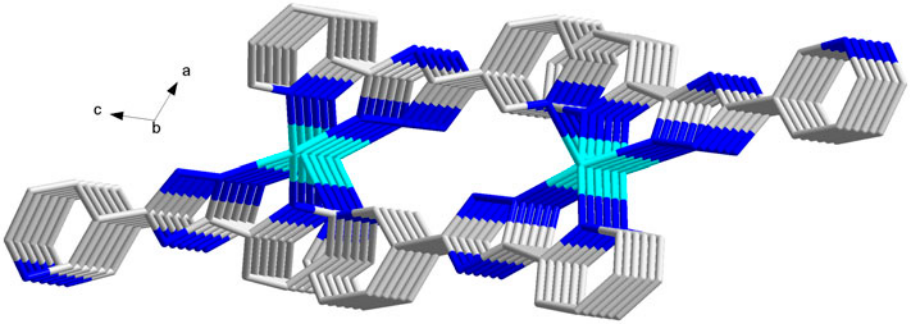

Figure 3. The 1-D channel along the *ac* plane.

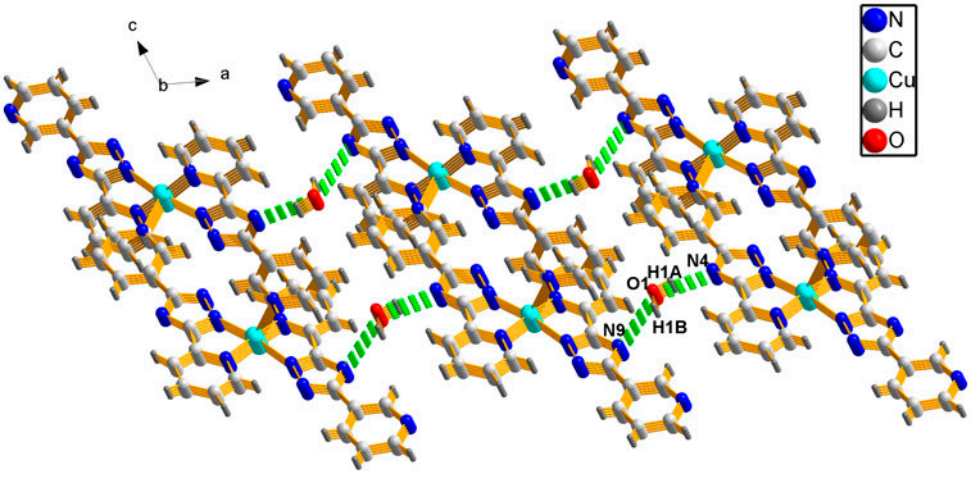

Figure 4. 2-D structure formed by hydrogen-bond interactions.

Table 3. Hydrogen-bonding interactions for **1**.

D–H···A	D–H (Å)	H···A (Å)	D···A (Å)	⟨DHA (°)
O1–H1A···N4	0.863	2.067	2.879	156.69
O1–H1B···N9#3	0.851	2.353	3.040	138.07

Note: Symmetry operations: #3 $x+1, y, z$.

From figure 4, we can see that there are two weak hydrogen-bond interactions between lattice water and 2,3′-bpt$^-$ [O1–H1A···N4, O1–H1B···N9]. Those hydrogen-bond interactions not only contribute significantly to the stability of complex, but also link the 1-D channel into 2-D planes in the *ac* plane. Hydrogen-bond distances and angles are listed in table 3.

3.2. *Thermal decomposition process of complex*

Thermogravimetric experiments were conducted to study the thermal stability of **1**, which is an important parameter for energetic materials. As shown in figure 5, the TGA curve of **1** suggests the first weight loss of 3.68% from 364 to 414 K, corresponding to expulsion of the lattice water (Calcd 3.42%). The main framework remains intact until it is heated to 624 K, and then releases all the ligands completely from 624 to 860 K with an exothermic peak at 708 K, giving CuO as the final decomposition product with residue percent of 15.40% (Calcd 15.11%).

To confirm the stable framework of **1**, the original sample and processed sample with lattice water molecule removed were characterized by X-ray powder diffraction (XRPD) at room temperature. As shown in figure 6, the processed sample resulted in a slightly broadened XRPD pattern with similar peak positions to that of the original sample, which shows that the crystallinity of **1** is retained. Figure 7 shows XRPD patterns of the residual. It is

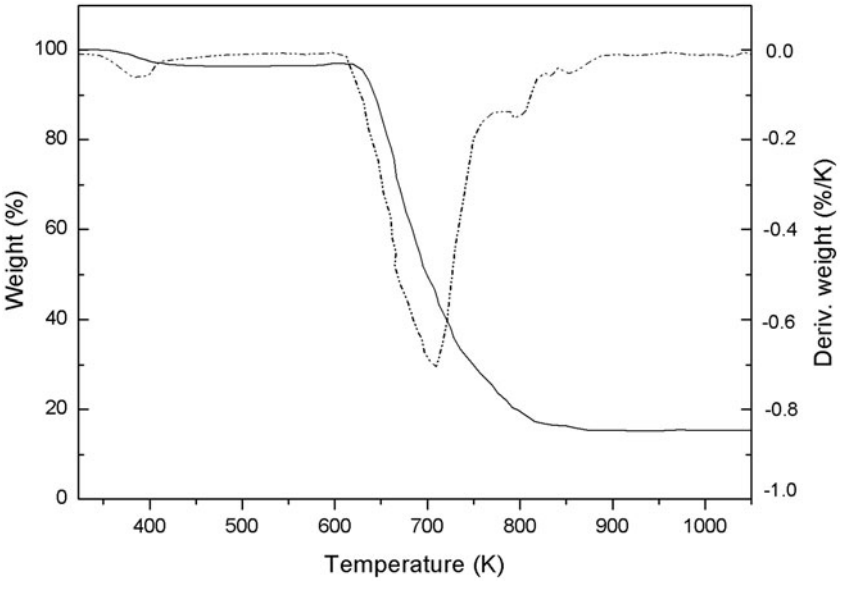

Figure 5. TGA curves for **1**.

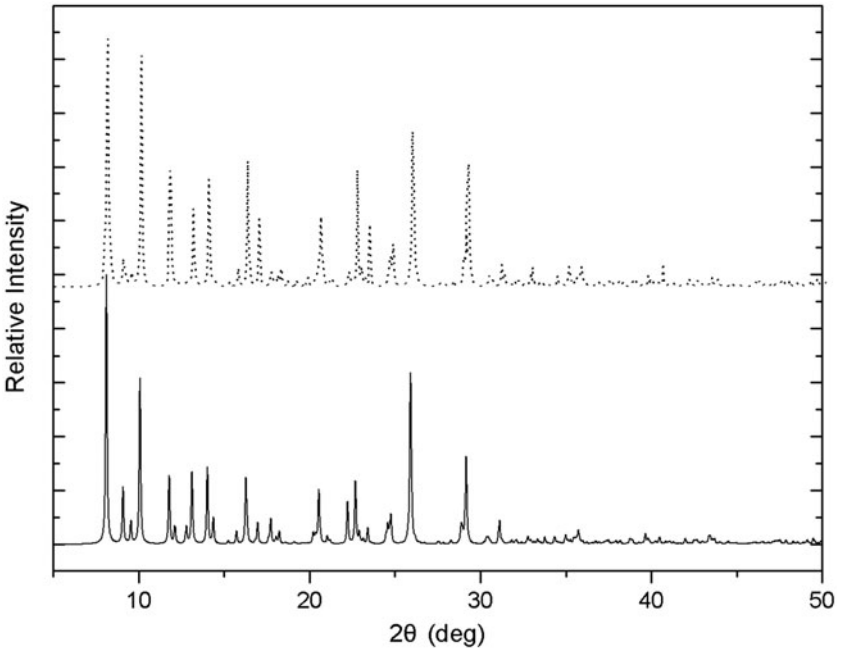

Figure 6. Comparison of XRPD patterns of the original sample and the desolvated phases: – , original sample; … , desolvated phases.

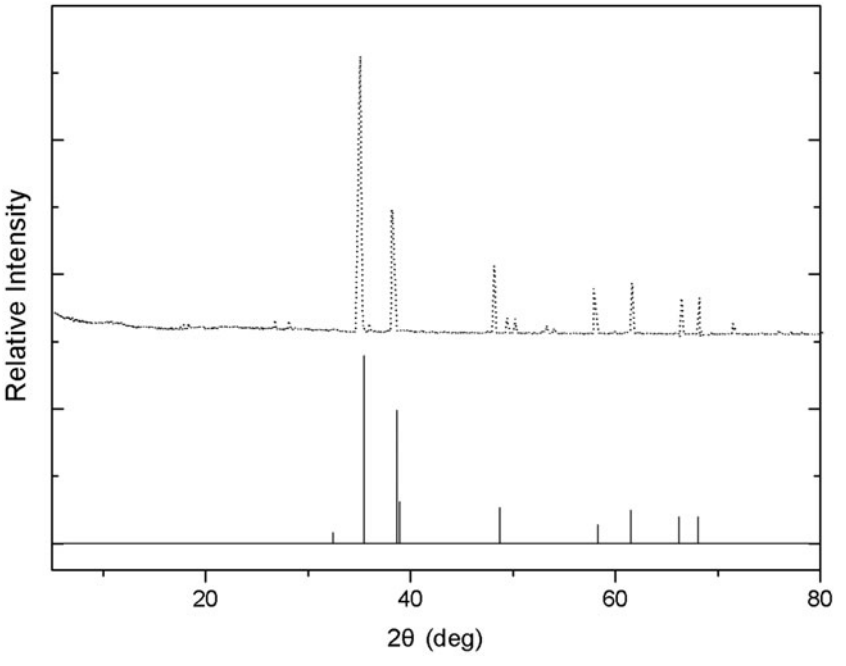

Figure 7. XPRD patterns of the residual: – , standard data for CuO; … , experimental data for the residual.

seen that all diffraction peaks are in good agreement with the standard diffraction data for CuO (JCPDS card file No. 45-0937).

3.3. *Effects on thermal decomposition of AP*

To check the effects on thermal decomposition of AP after adding the as-synthesized compound, AP and **1** are mixed at a mass ratio of 1 : 3 to prepare the target samples. The study is investigated by DSC measurement with a heating rate of 10 K min^{-1} in N_2 from 323 to 773 K with Al_2O_3 as reference. Figure 8 shows the DSC curves of AP, **1** and AP with **1**, respectively. The endothermic peak at 528 K for pure AP is attributed to the phase transformation, while the exothermic peaks at 563 and 715 K are corresponding to the low-temperature decomposition process and high-temperature decomposition process. The heat releases of exothermic process are 735 and 787 J g^{-1}, respectively. After adding the mixture of AP with **1**, there are no significant impacts on the phase transition of AP. While noticeable change can be seen in the exothermic phase. The two exothermic peaks merge to one and the temperature reduced to 573 K, which indicates a rapid decomposition process; the decomposition heat changes to 1946 J g^{-1}, significantly higher than the corresponding heat value for pure AP. Obviously, AP is completely decomposed in a shorter time and releases much heat in the presence of **1**. It can be inferred that the complex decomposes and releases heat itself, as well as the formation of metal and oxide at molecular level on propellant surface may contribute toward their catalytic effects [25].

The decomposition temperature is related with the heating rate. The relationship between decomposition temperature and heating rate can be described by the Kissinger correlation [26]. Kissinger's method is used to investigate the activation energy (E_a) and pre-exponential factor (A) of thermal decomposition for AP with additives by DSC measurement at four different heat rates of 5, 10, 15, and 20 K min^{-1} (figure 9),

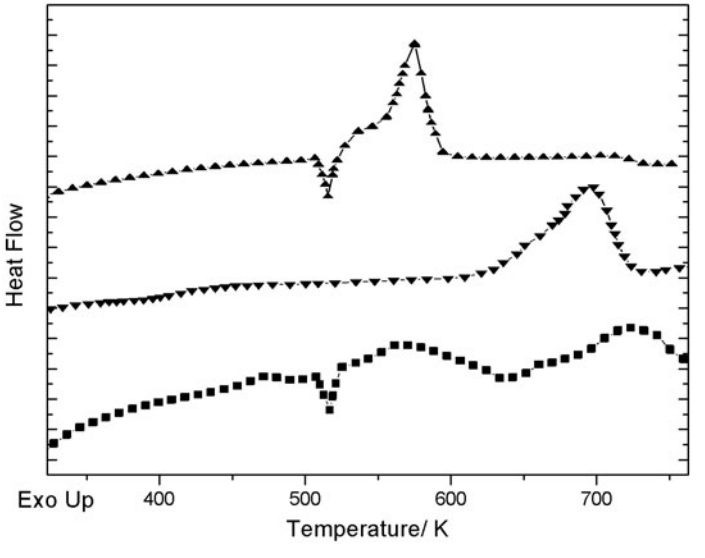

Figure 8. DSC curves for AP, AP with additives at a heating rate of 10 K min^{-1}.

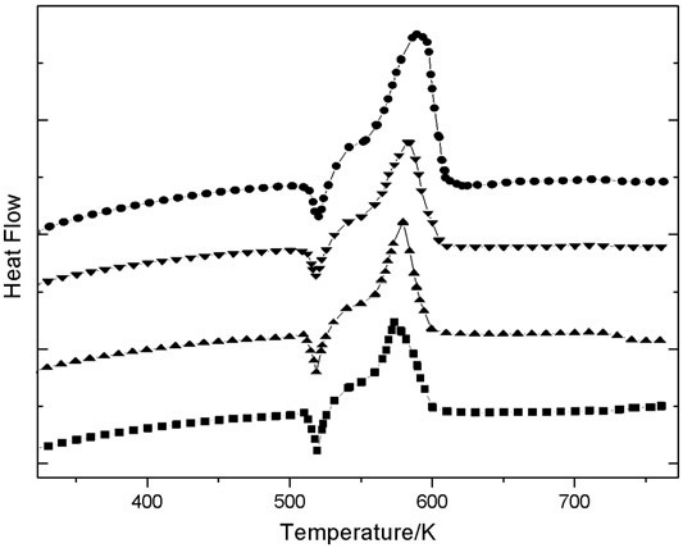

Figure 9. DSC curves of AP with additives at various heating rates: ■, $\beta = 5\ \mathrm{K\ min^{-1}}$; ▲, $\beta = 10\ \mathrm{K\ min^{-1}}$; ▼, $\beta = 15\ \mathrm{K\ min^{-1}}$; and ●, $\beta = 20\ \mathrm{K\ min^{-1}}$.

$$\ln\frac{\beta}{T_p^2} = \ln\frac{AR}{E_a} - \frac{E_a}{RT_p}$$

where β is the heating rate, R is the gas constant, and T_p is the peak temperature. As shown in table 4, the calculated activation energy E_a of pure AP is $74.65\ \mathrm{kJ\ M^{-1}}$. With the presence of complex, the activation energies change to $223.54\ \mathrm{kJ\ M^{-1}}$. Many researchers have reported a higher activation energy (E_a) for catalyzed AP than that of pure AP [18, 27, 28]. It is contrary to the generally observed trend of lowering E_a for a reaction whose rate is increased by a catalyst. This may be attributed to facts like strong interaction and binding between AP and the title complex and secondly along with E_a the pre-exponential factor (A) also showed variations. In a reaction catalyzed by a catalyst, there is an increase in reactant concentration at the catalyst surface, as confirmed earlier by observing high heat release. Thus, the reaction gets accelerated through a relatively high pre-exponential factor (A) in the presence of **1** ($\ln(A) = 18.27$) compared to pure AP ($\ln(A) = 5.71$) (table 4). As a result, a direct correlation of E_a with the reaction rate becomes difficult since both E_a and A are altered in the reaction. Thus the pre-exponential factor plays an important role in increasing the reaction rate of the thermal decomposition of AP. The increase in activation

Table 4. Kinetic parameters of thermal decomposition for AP and AP with additives (ΔH was given at the heating rate of $10\ \mathrm{K\ min^{-1}}$).

	ΔH/J g^{-1}	E_a/kJ M^{-1}	ln (A)	E_a/ln (A)
AP	735	74.65	5.71	13.07
AP + 1	1946	223.54	18.27	12.23

energy and the corresponding increase in the A value are due to the kinetic compensation effect as reported [18] and the ratio of $E_a/\ln(A)$ could be used to describe the reactivity [29]. Usually, a bigger ratio means a greater stability of the reactant. The ratios of $E_a/\ln(A)$ are 13.07 and 12.23 for pure AP and the mixture, respectively. The title complex shows good catalytic activity toward AP decomposition, which indicates potential application in solid propellants.

Comparing to other energetic complexes [9, 21, 30–33] which are the candidates of catalysts for the decomposition of AP, the complexes should meet the following requirements. First, the energetic ligands in these complexes could enhance the decomposition heats which are beneficial for thermal decomposition of AP. Second, the formation of metal and oxide at the molecular level on the propellant surface when the compounds decompose may contribute to the catalytic effect.

4. Conclusion

Complex **1** has been synthesized and the structure was determined by single-crystal X-ray diffraction as a zigzag chain along the (110) direction and a 1-D channel in the *ac* plane. Hydrogen-bond interactions link the channel into 2-D planes. With the heating rate of $10\,K\,min^{-1}$ under static air, the lattice water molecules were lost from 364 to 414 K and decomposition of $[Cu(2,3'\text{-bpt})_2]_n$ starts at 624 K with a sharp exothermic peak in TG-DTG curves. DSC experiment revealed that the two exothermic peaks for AP merged to one with the presence of **1** and the decomposition temperature reduced from 715 to 573 K, which indicates a rapid decomposition process. The decomposition heat changes to $1946\,J\,g^{-1}$, significantly higher than the corresponding heat value for pure AP. The kinetic parameters were studied by Kissinger's method. The ratios of $E_a/\ln(A)$ are 13.07 and 12.23 for pure AP and the mixture, which is a direct indication of the enhancement in the catalytic activity in the presence of **1**. The present study indicates probable application of the complex in solid propellant field. Further investigation is currently underway.

Supplementary material

CCDC 947187 contains the supplementary crystallographic data for this paper. These data can be obtained free of charge at http://www.ccdc.ac.uk/conts/retrieving.html or from the Cambridge Crystallographic Data Center (CCDC), 12 Union Road, Cambridge CB21EZ, UK; Fax: +44 1223 336033; E-mail: deposit@ccdc.cam.ac.uk.

Funding

We gratefully acknowledge the financial support from the National Natural Science Foundation of China [grant number 21263019], the Natural Science Foundation of Ningxia [grant number NZ12118] and Natural Science Foundation of the Ningxia University [grant number ZR1104].

References

[1] D.E. Chavez, M.A. Hiskey, R.D. Gilardi. *Angew. Chem. Int. Ed.*, **39**, 1791 (2000).
[2] W. Fraenk, T. Habereder, A. Hammerl, T.M. Klapötke, B. Krumm, P. Mayer, H. Nöth, M. Warchhold. *Inorg. Chem.*, **40**, 1334 (2001).
[3] H. Xue, H.X. Gao, B. Twamley, J.M. Shreeve. *Chem. Mater.*, **19**, 1731 (2007).
[4] D. Jones, K. Armstrong, T. Parekunnel, Q. Kwok. *J. Therm. Anal. Calorim.*, **86**, 641 (2006).
[5] B.D. Xue, Q. Yang, S.P. Chen, S.L. Gao. *J. Therm. Anal. Calorim.*, **101**, 997 (2010).
[6] G. Singh, R. Prajapati, R. Frohlich. *J. Hazard. Mater.*, **118**, 75 (2005).
[7] W.T. Wang, S.P. Chen, S.L. Gao. *Eur. J. Inorg. Chem.*, **2009**, 3475 (2009).
[8] D.M. Badgujar, M.B. Talawar, S.N. Asthana, P.P. Mahulikar. *J. Hazard. Mater.*, **151**, 289 (2008).
[9] B. Li, Q. Wei, Q. Yang, S.P. Chen, S.L. Gao. *J. Chem. Eng. Data*, **56**, 3043 (2011).
[10] L.M. Fan, D.C. Li, P.H. Wei, P.Q. Tang, M.H. Li, D. Yuan, G.Z. Liu, X.T. Zhang, J.M. Dou. *J. Coord. Chem.*, **64**, 3031 (2011).
[11] M. Tang, W. Guo, S.Z. Zhang, M. Du. *Inorg. Chem. Commun.*, **14**, 1217 (2011).
[12] W.Q. Kan, J. Yang, Y.Y. Liu, J.F. Ma. *CrystEngCommun.*, **14**, 6934 (2012).
[13] B. Li, S.P. Chen, Q. Yang, S.L. Gao. *Polyhedron*, **30**, 1213 (2011).
[14] B. Li, S.P. Chen, G. Xie, Q. Yang, S.L. Gao. *Struct. Chem.*, **23**, 417 (2012).
[15] L.J. Chen, L.P. Li, G.S. Li. *J. Alloys Compd.*, **464**, 532 (2008).
[16] V.V. Boldyrev. *Thermochim. Acta*, **443**, 1 (2006).
[17] T.M. Fu, F.Q. Liu, L. Liu, L.W. Guo, F.S. Li. *Catal. Commun.*, **10**, 108 (2008).
[18] L.P. Li, X.F. Sun, X.Q. Qiu, J.X. Xu, G.S. Li. *Inorg. Chem.*, **47**, 8839 (2008).
[19] X.F. Sun, X.Q. Qiu, L.P. Li, G.S. Li. *Inorg. Chem.*, **47**, 4146 (2008).
[20] G. Singh, S.P. Felix. *Combust. Flame*, **132**, 422 (2003).
[21] Q. Yang, S.P. Chen, G. Xie, S.L. Gao. *J. Coord. Chem.*, **65**, 2584 (2012).
[22] Q. Yang, S.P. Chen, S.L. Gao. *Inorg. Chem. Commun.*, **12**, 1224 (2009).
[23] G. Xie, B. Li, S.P. Chen, Q. Yang, W. Wei, S.L. Gao. *Sci. China, Ser. B Chem.*, **55**, 443 (2012).
[24] E. Browne. *Aust. J. Chem.*, **28**, 2543 (1975).
[25] P.B. Kulkarni, T.S. Reddy, J.K. Nair, A.N. Nazare, M.B. Talawar, T. Mukundan, S.N. Asthana. *J. Hazard. Mater.*, **123**, 54 (2005).
[26] H.E. Kissinger. *J. Anal. Chem.*, **29**, 1702 (1957).
[27] P.R. Patil, V.N. Krishnamurthy, S.S. Joshi. *Propellants Explos. Pyrotech.*, **31**, 442 (2006).
[28] R. Rajeev, C. Gopalkrishnan, K. Krishnan, K.G. Kannan, K.N. Ninan. In *3rd International High Energy Materials Conference and Exhibition (HEMCE)*, Thiruvananthapuram, India, 121 (2000).
[29] B. Andričić, T. Kovačić, I. Klarić. *Polym. Degrad. Stab.*, **79**, 265 (2003).
[30] Q. Yang, S.P. Chen, G. Xie, S.L. Gao. *J. Coord. Chem.*, **65**, 2584 (2012).
[31] X.B. Zhang, Y.H. Ren, W. Li, F.Q. Zhao, J.H. Yi, B.Z. Wang, J.R. Song. *J. Coord. Chem.*, **66**, 2551 (2013).
[32] F. He, K.Z. Xu, H. Zhang, Q.Q. Qiu, J.R. Song, F.Q. Zhao. *J. Coord. Chem.*, **66**, 845 (2013).
[33] Z.M. Li, T.L. Zhang, L. Yang, Z.N. Zhou, J.G. Zhang. *J. Coord. Chem.*, **65**, 143 (2012).